

This is the accepted manuscript made available via CHORUS. The article has been published as:

Virtual photon polarization in ultrarelativistic heavy-ion collisions

Gordon Baym, Tetsuo Hatsuda, and Michael Strickland

Phys. Rev. C **95**, 044907 — Published 14 April 2017

DOI: [10.1103/PhysRevC.95.044907](https://doi.org/10.1103/PhysRevC.95.044907)

Virtual photon polarization in ultrarelativistic heavy-ion collisions

Gordon Baym,^{a,b} Tetsuo Hatsuda,^{b,c} and Michael Strickland^d

^a*Department of Physics, University of Illinois, 1110 W. Green Street, Urbana, IL 61801-3080, United States*

^b*iTHES Research Group and iTHEMS Program, RIKEN, Wako, Saitama 351-0198, Japan*

^c*Nishina Center, RIKEN, Wako, Saitama 351-0198, Japan*

^d*Department of Physics, Kent State University, Kent, OH 44242, United States*

The polarization of direct photons produced in an ultrarelativistic heavy-ion collision reflects the momentum anisotropy of the quark-gluon plasma created in the collision. This paper presents a general framework, based on the photon spectral functions in the plasma, for analyzing the angular distribution and thus the polarization of dileptons in terms of the plasma momentum anisotropies. The rates of dilepton production depend, in general, on four independent spectral functions, corresponding to two transverse polarizations, one longitudinal polarization, and – in plasmas in which the momentum anisotropy is not invariant under parity in the local rest frame of the matter – a new spectral function, ρ_n , related to the anisotropy direction in the collision. The momentum anisotropy appears in the difference of the two transverse spectral functions, as well as in ρ_n . As an illustration, we delineate the spectral functions for dilepton pairs produced in the lowest order Drell-Yan process of quark-antiquark annihilation to a virtual photon.

PACS numbers: 25.75.Cj, 12.38.Mh, 11.10.Wx

I. INTRODUCTION

Direct photons, both real and virtual, are an important probe of the dynamics of ultrarelativistic heavy-ion collisions. An average temperature of the quark-gluon plasma (QGP) formed in high-energy collisions has been extracted from the transverse momentum spectrum of direct photons in the range $q_T \sim 1\text{--}3$ GeV [1–3]. Theoretically, measurements of the photon polarization through the angular distribution of dileptons (l^+l^-) have been proposed to provide information on the early stages of collisions, before the onset of thermalization [4–6]. While relativistic hydrodynamics provides a successful space-time description of the later stages of the collision dynamics and associated hadronic and leptonic observables [7], important questions concerning the early dynamics, such as the degree of thermalization as well as isotropization of the QGP, have not been answered either experimentally or theoretically. Recently, Ref. [8] proposed using the polarization of direct photons as a measure of the gluon anisotropy in collisions. While measuring direct photon polarization, involving external conversion to dilepton pairs, is very difficult experimentally, a more promising approach is to measure polarization of virtual photons, through the angular distribution of dileptons produced via internal conversion.

The lowest order mechanism to produce dilepton pairs is the Drell-Yan process, Fig. 1, in which a quark and an antiquark annihilate to a virtual photon. The dilepton cross section $d\sigma/d\Omega$ can be parametrized as $\propto 1 + \lambda \cos^2 \theta + \mu \sin 2\theta \cos \phi + (\nu/2) \sin^2 \theta \cos 2\phi$, where θ and ϕ are the polar and azimuthal angles of one of the dileptons in the dilepton rest frame measured in the Collins-Soper reference frame [9, 10]. High-energy $p\bar{p}$ and pp collisions at the Tevatron and the LHC have confirmed the leading-order prediction $\lambda \simeq 1$, $\mu = \nu = 0$, for $q_T \lesssim 5$ GeV and invariant dilepton mass $M_{l^+l^-} \simeq M_Z$ (see, e.g., [11] and

references therein). The dilepton angular distribution in In-In collisions has been measured by the NA60 experiment [12] at the CERN-SPS in the primary kinematical range $0.4 < M_{l^+l^-} < 0.9$ GeV, in which production of dileptons by hadronic sources such as $\pi^+\pi^-$ annihilation dominates Drell-Yan dileptons; the results are consistent with $\lambda = \mu = \nu = 0$.

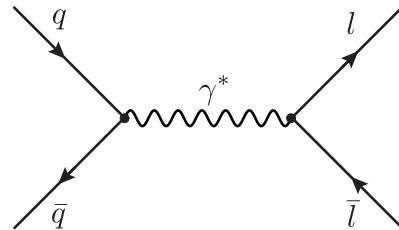


FIG. 1: Lowest order Drell-Yan production of a lepton pair.

On the other hand, in ultrarelativistic heavy-ion collisions we expect the momentum-space anisotropy of the QGP to be detected most readily in dilepton production in the range $1 \text{ GeV} < q_T < 3 \text{ GeV}$ and $M_{l^+l^-} \lesssim 0.3 \text{ GeV}$ where the excess of direct photons is seen experimentally [1]. In this paper, we present a general framework for analyzing the angular distribution of dileptons emitted from a QGP, which can be used to extract quark and gluon momentum anisotropies in the collision. The basic starting point is the photon polarization tensor and associated spectral function; we analyze the spectral function in terms of four vectors, two transverse polarization vectors, a longitudinal polarization vector, and a vector specifying the momentum anisotropy. Such a decomposition combined with the leptonic tensor describing the conversion of a virtual photon into a dilepton pair leads to a general formula relating the momentum anisotropy of the plasma and the dilepton angular distribution. As

an illustration, we apply the formalism to virtual photon emission through the leading-order Drell-Yan process in a plasma with anisotropic distributions of the Romatschke-Strickland form [13].¹

II. DILEPTON PRODUCTION

Quite generally, the production rate, R , of a dilepton pair is proportional to the spectral function, $\rho_{\mu\nu}$, of the in-medium photon polarization or self-energy operator, for momentum \vec{q} and energy q^0 ,

$$\Pi_{\mu\nu}(\vec{q}, z) = e^2 \int_{-\infty}^{\infty} \frac{dq^0}{2\pi} \frac{\rho_{\mu\nu}(\vec{q}, q^0)}{z - q^0}, \quad (1)$$

times the squared matrix element $L^{\mu\nu}$ (L for leptons) for a virtual photon of 4-momentum q to produce a lepton of 4-momentum p and mass m and an antilepton of 4-momentum p' , averaged over the spins of the leptons. Explicitly,

$$\frac{dR_{l+l^-}}{d^3\vec{p}d^3\vec{p}'} = \frac{\alpha^2}{4\pi^4 Q^4} \rho_{\mu\nu}(q) L^{\mu\nu}(p, p'), \quad (2)$$

with the leptonic tensor,

$$L_{\mu\nu}(q, s) = 2(q_\mu q_\nu - g_{\mu\nu} Q^2 - s_\mu s_\nu), \quad (3)$$

where $d^3\vec{p} \equiv d^3p/2E_p$, $d^3\vec{p}' \equiv d^3p'/2E_{p'}$, $q = p + p'$, $s = p - p'$, $Q^2 \equiv q^\mu q_\mu > 0$, and $Q^2 + s^2 = 4m^2$ with m the lepton mass.

The spectral function $\rho_{\mu\nu}(q)$ is related to the cut, or imaginary part, of the photon polarization operator, illustrated in Fig 2. Its explicit form in the kinematical regime $q^0 \gg T \gg \sqrt{Q^2}$ has been previously evaluated using hard thermal loop effective theory for the isotropic quark-gluon plasma [15, 16]. The heart of the problem in this paper is to determine the structure of $\rho_{\mu\nu}(q)$, to see how the anisotropy of the gluon and quark distributions is reflected in the final orientation of the dilepton pair.

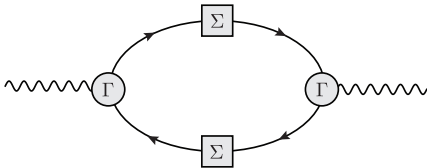


FIG. 2: Photon polarization tensor with hard thermal loop corrections to the quark lines and vertices [15].

¹ In the course of writing this paper we became aware of the work of Friman and collaborators [14] which does not include the anisotropic terms $\rho_1^T - \rho_2^T$ and ρ_n , but otherwise arrives at results in agreement with those given here; the approach of these two treatments of the problems are complementary and will be discussed in a future joint publication of the two groups.

III. STRUCTURE OF $\rho_{\mu\nu}$

In a heavy-ion collision volume, the initial gluon and quark distributions are anisotropic in momentum space with a single preferred axis \hat{n} , which we assume to be along the beam direction [17] (we do not consider at this point possible multiple anisotropy axes). We define the four vector n^μ to have space component \hat{n} in the local rest frame of the matter and time component, $n^0 = 0$,

$$n^\mu = (0, \hat{n}), \quad (4)$$

so that $n^2 = -1$. We also define, in the local rest frame, the two transverse polarization vectors

$$\varepsilon_i^\mu = (0, \hat{\varepsilon}_i), \quad (5)$$

where $\hat{\varepsilon}_1 \equiv (\vec{q} \times \hat{n}) \times \vec{q}/|\vec{q} \times \hat{n}|$ and $\hat{\varepsilon}_2 \equiv \vec{q} \times \hat{n}/|\vec{q} \times \hat{n}|$. These polarization vectors are illustrated in the left panel of Fig. 3. In addition, we define the longitudinal polarization vector

$$\varepsilon_L^\mu \equiv \frac{1}{\sqrt{Q^2}}(|\vec{q}|, q^0 \hat{q}) = (|\vec{q}|, \vec{q}^0 \hat{q}). \quad (6)$$

where we write $\tilde{q}^\mu = q^\mu/\sqrt{Q^2}$. Note that $\varepsilon_1^2 = \varepsilon_2^2 = \varepsilon_L^2 = -1$. The three polarization vectors are individually orthogonal to q^μ : $(q\varepsilon) = 0$ (where (ab) denotes the four vector product of a and b) and together with q^μ form an orthogonal basis obeying;

$$g^{\mu\nu} = \tilde{q}^\mu \tilde{q}^\nu - \varepsilon_1^\mu \varepsilon_1^\nu - \varepsilon_2^\mu \varepsilon_2^\nu - \varepsilon_L^\mu \varepsilon_L^\nu. \quad (7)$$

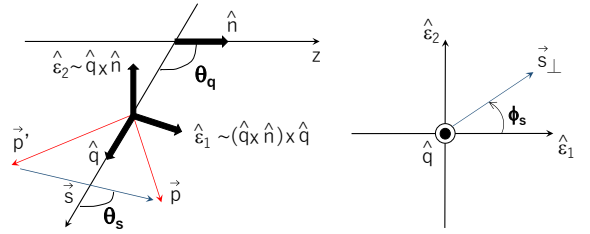


FIG. 3: (Left) Virtual photon polarization vectors $\hat{\varepsilon}_i$ and the relative spatial momentum \vec{s} between the lepton and antilepton. (Right) The relative lepton momentum in the plane transverse to the virtual photon momentum \vec{q} .

Thus the photon spectral function, $\rho_{\mu\nu}$, is a sum of terms of the form

$$a\varepsilon_L^\mu \varepsilon_L^\nu + b\varepsilon_1^\mu \varepsilon_1^\nu + c(\varepsilon_1^\mu \varepsilon_L^\nu + \varepsilon_L^\mu \varepsilon_1^\nu) + d\varepsilon_2^\mu \varepsilon_2^\nu. \quad (8)$$

There are no terms proportional to $q^\mu q^\nu$ for $Q^2 \neq 0$, since q is a zero eigenvector of ρ ; in addition $(n\varepsilon_2) = 0$,

so there are no $\varepsilon_2 \varepsilon_L$ terms by symmetry. Since \vec{n} can be written as the linear superposition, $\vec{n} = \cos \theta_q \hat{q} + \sin \theta_q \vec{\varepsilon}_2$, with θ_q being the angle between \hat{n} and \hat{q} , and $n^0 = 0$, we obtain

$$n^\mu = \cos \theta_q (\tilde{q}^0 \varepsilon_L^\mu - |\vec{q}| \tilde{q}^\mu) + \sin \theta_q \varepsilon_1^\mu. \quad (9)$$

We also introduce the four-vector \mathcal{N}^μ with the property $(\mathcal{N}q) = 0$ as,

$$\mathcal{N}^\mu \equiv \tilde{q}^0 \cos \theta_q \varepsilon_L^\mu + \sin \theta_q \varepsilon_1^\mu = n^\mu - (\tilde{q}n) \tilde{q}^\mu, \quad (10)$$

Thus the $\varepsilon_1^\mu \varepsilon_L^\nu + \varepsilon_L^\mu \varepsilon_1^\nu$ term can be eliminated in favor of $\mathcal{N}^\mu \mathcal{N}^\nu$, $\varepsilon_1^\mu \varepsilon_1^\nu$, and $\varepsilon_L^\mu \varepsilon_L^\nu$. In addition, $\mathcal{N}^2 = -(1 + (n\tilde{q})^2)$. The latter term, plus the explicit $\varepsilon_L^\mu \varepsilon_L^\nu$ term in Eq. (8), can be eliminated using Eq. (7). The photon spectral function, again with the help of Eq. (7), assumes the general form

$$\rho^{\mu\nu} = \varepsilon_L^\mu \varepsilon_L^\nu \rho_L + \varepsilon_1^\mu \varepsilon_1^\nu \rho_1^T + \varepsilon_2^\mu \varepsilon_2^\nu \rho_2^T + \mathcal{N}^\mu \mathcal{N}^\nu \rho_n \quad (11)$$

$$= -(g^{\mu\nu} - \tilde{q}^\mu \tilde{q}^\nu) \rho^L + \varepsilon_1^\mu \varepsilon_1^\nu (\rho_1^T - \rho^L) + \varepsilon_2^\mu \varepsilon_2^\nu (\rho_2^T - \rho^L) + \mathcal{N}^\mu \mathcal{N}^\nu \rho_n. \quad (12)$$

The momentum-space anisotropy of the system leads to the extra ρ_n term, as well as a difference of ρ_1^T and ρ_2^T .

The terms ρ_n , ρ_2^T can be extracted directly from Eqs. (11) and (10) as

$$\varepsilon_1 \mu \rho^{\mu\nu} \varepsilon_{L\nu} = -\tilde{q}^0 \cos \theta_q \sin \theta_q \rho_n, \quad (13)$$

and

$$\varepsilon_2 \mu \rho^{\mu\nu} \varepsilon_{2\nu} = \rho_2^T, \quad (14)$$

while ρ^L is found from

$$\varepsilon_{L\mu} \rho^{\mu\nu} \varepsilon_{L\nu} = \rho^L + (\tilde{q}^0)^2 \cos^2 \theta_q \rho_n. \quad (15)$$

Using Eq. (13), we find ρ_1^T from the trace condition,

$$\rho_\mu^\mu = -(\rho^L + \rho_1^T + \rho_2^T + (1 + (n\tilde{q})^2) \rho_n). \quad (16)$$

When the particle distribution functions are even under parity, so that \vec{n} enters only as a special axis, not a special direction, the extra ρ_n term must vanish. To see this we note that when the distribution functions are parity invariant, both parity and the transformation $\hat{n} \rightarrow -\hat{n}$ are independent symmetries, meaning that a parity transformation keeping \vec{n} fixed is also a symmetry. But under such a transformation $\vec{\varepsilon}_L$ transforms as a vector, while $\vec{\varepsilon}_1$ transforms as a pseudovector; thus the mixing of the two directions in ρ_{ij} , the source of ρ_n , cannot occur. For collisions of two identical nuclei, there should not be a special direction in the local rest frame of the matter. Below, when we write down the Drell-Yan rate in the medium in such a situation, we will see explicitly how this argument is realized. However, for asymmetric collisions, one expects a non-zero ρ_n term in the photon spectral function. In the following, we keep the ρ_n term in the general discussions.

The various ρ depend separately on the local q^0 , q_\perp , and $\vec{q} \cdot \hat{n}$, where q_\perp is the magnitude of the component of \vec{q} orthogonal to \hat{n} . Or expressed covariantly, they depend on Q^2 , (qu) , as well as on (qn) , where u_μ is the 4-velocity of the local rest frame. Note that $(nu) \equiv 0$.

We look now at the eigenvalue structure of photon spectral function. In the local rest frame, in an isotropic system or for \vec{q} along \hat{n} , the ρ_n term vanishes and $\rho_1^T = \rho_2^T$, while for $\vec{q} \perp \hat{n}$ the eigenvectors of ρ are the ε_i , with the two eigenvalues, ρ_1^T and ρ_2^T . More generally, in the local rest frame, the eigenvectors of $\rho^{\mu\nu}$ are q^μ with eigenvalue 0, ε_2^μ with eigenvalue ρ_2^T , and two orthogonal linear combinations of ε_1^μ and ε_L^μ whose spatial components lie in the (\vec{q}, \hat{n}) plane. In the isotropic limit, the eigenvector ε_L has eigenvalue ρ_L , and ε_1 has eigenvalue ρ_T . In contrast, when the system is anisotropic, the two eigenfunctions describe propagation in a birefringent medium with a mixing of the longitudinal (L) and transverse (T) polarizations. Furthermore, as $\vec{q} \rightarrow 0$, $\rho_i^T - \rho^L$ must vanish as \vec{q}^2 , and thus, $\rho_i^T = \rho^L$ for $i = 1, 2$.

IV. EMISSION RATE OF DILEPTONS AND PHOTONS

To calculate the production rates of dilepton pairs we first note that quite generally, $(sq) = 0$, so that

$$\frac{1}{2} \rho^{\mu\nu} L_{\mu\nu} = -(Q^2 \rho_\mu^\mu + s_\mu \rho^{\mu\nu} s_\nu) \quad (17)$$

$$= Q^2 (\rho_1^T + \rho_2^T + \rho_n) + 4m^2 \rho^L - s_1^2 (\rho_1^T - \rho^L) - s_2^2 (\rho_2^T - \rho^L) + ((qn)^2 - (sn)^2) \rho_n, \quad (18)$$

where we use the identity $Q^2 + s^2 = 4m^2$, with m being the lepton mass, and we define $s_i \equiv (s\varepsilon_i)$ ($i = 1, 2$) to be the components of \vec{s} transverse to \vec{q} in the local rest frame: $\vec{s}_\perp = s_1 \vec{\varepsilon}_1 + s_2 \vec{\varepsilon}_2$.

Equation (18) gives the dilepton production rate in terms of the projections of s along the two transverse polarizations and n . The s_1^2 and s_2^2 terms contain the anisotropy produced by transverse virtual photons, while from Eq. (9), we see that the s_z^2 term arises from the mixing of longitudinal and transverse ($\vec{\varepsilon}_1$) virtual photons. As noted above, for symmetric collisions with parity invariance in the local matter rest frame, ρ_n should vanish so then the final term Eq. (18) is absent. To bring out the anisotropic terms, we write $s_1 = |\vec{s}_\perp| \cos \phi_s$, and $s_2 = |\vec{s}_\perp| \sin \phi_s$; the squared matrix elements (18) become

$$\begin{aligned} \frac{1}{2} \rho^{\mu\nu} L_{\mu\nu} = & 2Q^2 \bar{\rho}^T + (s_\perp^2 + 4m^2) \rho^L \\ & + (Q^2 + (qn)^2 - (sn)^2) \rho_n \\ & - |\vec{s}_\perp|^2 (\bar{\rho}^T + \delta \rho^T \cos 2\phi_s), \end{aligned} \quad (19)$$

where $\bar{\rho}^T \equiv (\rho_1^T + \rho_2^T)/2$ and $\delta \rho^T \equiv (\rho_1^T - \rho_2^T)/2$. The $\cos 2\phi_s$ as well as the ρ_n terms are anisotropic. For

massless dileptons in the absence of ρ_n , the right side of Eq. (19) becomes $2Q^2 \bar{\rho}^T + |\vec{s}_\perp|^2 (\rho^L - \bar{\rho}^T - \delta\rho^T \cos 2\phi_s)$. With θ_s the angle between \vec{q} and \vec{s} , we see that this expression is of the form $\propto 1 + \lambda_s \cos^2 \theta_s + \mu_s \sin 2\theta_s \cos \phi_s + (\nu_s/2) \sin^2 \theta_s \cos 2\phi_s$, with

$$\lambda_s = \frac{\bar{\rho}^T - \rho^L}{\bar{\rho}^T(1 - 2s_0^2/\bar{s}^2) + \rho^L},$$

$$\nu_s = \frac{-2\delta\rho^T}{\bar{\rho}^T(1 - 2s_0^2/\bar{s}^2) + \rho^L}, \quad (20)$$

and $\mu_s = 0$. We note the similarity to the angular distribution fitted in the NA60 analysis [12], where the angles are defined in the Collins-Soper frame; as noted above, NA60 finds when averaging over all lab directions of the virtual photons, that λ , μ , and ν are consistent with zero.

With the Jacobian from the variables p and p' to Q , \vec{s}_\perp , rapidity y and \vec{q}_T ,

$$d^3\bar{p} d^3\bar{p}' = \frac{1}{2} \frac{dQ^2 dy d^2q_T d^2s_\perp}{\sqrt{Q^2(Q^2 - s_\perp^2 - 4m^2)}}, \quad (21)$$

we finally obtain the dilepton emission rate

$$\frac{dR_{l+l-}}{dQ^2 d^2s_\perp dy d^2q_T} = \frac{\alpha^2}{4\pi^4 Q^4} \frac{\rho^{\mu\nu} L_{\mu\nu}/2}{\sqrt{Q^2(Q^2 - s_\perp^2 - 4m^2)}}, \quad (22)$$

where $\rho^{\mu\nu} L_{\mu\nu}/2$ is given by Eq. (19). As seen in Fig. 3, the components (sn) and (qn) are not independent; their dependence on the experimental variables, Q^2 , s_\perp , y , and q_T is algebraic (but too complicated to quote here).

It is instructive to connect the present formalism for virtual photons to the calculation of the rate for real photons, $Q^2 = 0$ including possible polarization, as considered by [18, 19] and [8]. To do so, we rewrite Eq. (12) as

$$\rho^{\mu\nu} = -(g^{\mu\nu} Q^2 - q^\mu q^\nu) \frac{\rho^L}{Q^2} + \varepsilon_1^\mu \varepsilon_1^\nu (\rho_1^T - \rho^L)$$

$$+ \varepsilon_2^\mu \varepsilon_2^\nu (\rho_2^T - \rho^L) + (Q^2 \mathcal{N}^\mu)(Q^2 \mathcal{N}^\nu) \frac{\rho_n}{Q^4}, \quad (23)$$

from which we see that as $Q^2 \rightarrow 0$, ρ_L vanishes as Q^2 and ρ_n vanishes as Q^4 . Thus the rate to produce a real photon with polarization ε^μ is

$$\frac{dR_\gamma}{d^3\vec{q}} = \frac{\alpha}{2\pi^2} \varepsilon_\mu^* \rho^{\mu\nu} \varepsilon_\nu,$$

$$= \frac{\alpha}{2\pi^2} (\bar{\rho}^T + (|\varepsilon\varepsilon_1|^2 - |\varepsilon\varepsilon_2|^2) \delta\rho^T)$$

$$= \frac{\alpha}{2\pi^2} (\bar{\rho}^T + \delta\rho^T \cos 2\phi_\varepsilon), \quad (24)$$

where $(\varepsilon\varepsilon_1) \equiv -\cos \phi_\varepsilon$, $(\varepsilon\varepsilon_2) \equiv -\sin \phi_\varepsilon$, and $d^3\vec{q} = d^3q/2|\vec{q}|$. The anisotropy for real photons arises entirely from the difference, $\delta\rho^T$, of ρ_1^T and ρ_2^T : the spectral function ρ_n does not enter.

V. DRELL-YAN PROCESS IN THE MEDIUM

To give a specific illustration of the present formalism we focus on the leading-order Drell-Yan production of dilepton pairs where the squared matrix element for a quark and antiquark to produce a virtual photon is

$$H_{\mu\nu}(q, t) = 2(q_\mu q_\nu - g_{\mu\nu} Q^2 - t_\mu t_\nu), \quad (25)$$

with $t = k - k'$ the difference of the four momenta of the two incident quarks, k and k' .

In a heavy-ion collision, the anisotropy in the Drell-Yan process arises only from the distributions of the initial quarks and antiquarks. The imaginary part of the lowest-order photon polarization tensor in a heavy-ion collision is

$$\frac{1}{2} \rho^{\mu\nu}(q) = (q_\mu q_\nu - g_{\mu\nu} Q^2) \langle 1 \rangle - \langle t_\mu t_\nu \rangle, \quad (26)$$

where

$$\langle X \rangle = N_c \sum_f \frac{e_f^2}{4\pi^2} \int d^3\vec{k} d^3\vec{k}' X \delta^{(4)}(q - k - k') f_{\vec{k}} \bar{f}_{\vec{k}'}, \quad (27)$$

with the sum being over flavors, e_f denoting the quark charge; $+2/3$ for u -quarks, $-1/3$ for d -quarks, etc., and $N_c = 3$ is the number of colors. The generally anisotropic quark and antiquark distributions are denoted by f and \bar{f} , respectively.²

In this notation, the coefficients in the spectral distribution function are obtained by comparing Eqs. (11) and (26):

$$\rho_1^T + \sin^2 \theta_q \rho_n = 2Q^2 \langle 1 \rangle - 2\langle (\varepsilon_1 t)^2 \rangle,$$

$$\rho_2^T = 2Q^2 \langle 1 \rangle - 2\langle (\varepsilon_2 t)^2 \rangle,$$

$$\rho^L + (\bar{q}^0)^2 \cos^2 \theta_q \rho_n = 2Q^2 \langle 1 \rangle - 2\langle (\varepsilon_L t)^2 \rangle, \quad (28)$$

with

$$\rho_n = -\frac{4}{\bar{q}^0 \sin 2\theta_q} \langle (\varepsilon_1 t)(\varepsilon_L t) \rangle. \quad (29)$$

When the product of the distribution functions is invariant under parity as well as $\hat{n} \rightarrow -\hat{n}$, ρ_n must vanish, as argued after Eq. (16). Explicitly, the orthogonality $(qt) = 0$ implies $(\varepsilon_L t) = -t^0/|\vec{q}|$, so that in Eq. (29), $\langle \varepsilon_1 t(\varepsilon_L t) \rangle \sim \vec{\varepsilon}_1 \cdot \langle t^0 \vec{t} \rangle$. But $\langle t^0 \vec{t} \rangle$ can at most be proportional to a linear combination of \vec{q} and \hat{n} , and if $\hat{n} \rightarrow -\hat{n}$ is

² The photon polarization operator is not that for an equilibrium system at finite temperature, owing to the fact that the electromagnetic sector in a heavy-ion collision never has adequate time to come into thermal equilibrium. The inverse processes in which a dilepton pair is absorbed, would lead to the distributions entering as $f_{\vec{k}} \bar{f}_{\vec{k}'} + (1 - f_{\vec{k}})(1 - \bar{f}_{\vec{k}'}) = 1 - f_{\vec{k}} - \bar{f}_{\vec{k}'}$ in the thermal equilibrium photon spectral function in full thermal equilibrium.

an invariance, the \hat{n} term must vanish; then since $\vec{q} \cdot \vec{\varepsilon}_1 = 0$ one has $\rho_n = 0$. In this case, Eq. (28) implies

$$\delta\rho^T = -\langle(\vec{\varepsilon}_1 \cdot \vec{t})^2 - (\vec{\varepsilon}_2 \cdot \vec{t})^2\rangle = -\frac{3}{2}\langle t_z^2 - \vec{t}^2/3\rangle \sin^2\theta_q, \quad (30)$$

which has the structure of a second spherical harmonic, and will thus select out the second spherical harmonic anisotropy in the particle distribution functions.

A simple approach to describing the anisotropy of the distributions is to assume an angular dependent temperature, so that, e.g., the quark distribution of massless quarks becomes (with the chemical potential suppressed)

$$f_{\vec{k}} = \frac{1}{e^{\beta(\hat{k})k} + 1}. \quad (31)$$

The parametrization of the angular dependent inverse temperature given in Ref. [13] takes the form $\beta(\hat{k}) = \beta_0(1 + \xi \cos^2\theta_k)^{1/2}$ where θ_k is the angle between the quark momentum \vec{k} and the anisotropy (z) axis. The full calculation of the Drell-Yan dileptons in an ultra-relativistic heavy-ion collisions with such an anisotropic temperature has been given by Strickland et al. [20–23].

To illustrate, we expand the quark distribution functions, assumed to be of the form Eq. (31), to lowest order in the angular dependence of the temperature, writing

$$f_{\vec{k}} \simeq f_k^0 - f_k^0(1 - f_k^0)(\beta(\hat{k}) - \beta_0)k, \quad (32)$$

where f_k^0 is the distribution with $\beta(\hat{k}) = \beta_0$. We see then that for weak anisotropy,

$$\delta\rho^T \sim -\frac{3}{2}\langle t_z^2 - \vec{t}^2/3\rangle \sim -\beta_2 \quad (33)$$

where $\beta_2 = \frac{1}{2} \int_{-1}^1 d(\cos\theta) \beta(\hat{k}) P_2(\cos\theta) = \beta_0 \xi/15$ is the second spherical harmonic component of the temperature.

The terms in the photon spectral function $\rho_{\mu\nu}$ beyond the lowest order Drell-Yan contribution are found from the imaginary part of the polarization diagram in Fig. 2 with hard thermal loop corrections and distribution anisotropies [24].

In practice, in order to obtain the dilepton spectra, one should integrate the spectral function, as given by Eq. (27), over the space-time volume of the collision volume with an underlying model for the dynamics of $\xi(x)$ and $\beta_0(x)$ such as viscous [25] or anisotropic hydrodynamics [26]. Previous work has shown that the high-energy dilepton rate computed in this manner is sensitive to the assumed initial momentum-space anisotropy of the plasma [23] and that the momentum-space anisotropy of the quark-gluon plasma induces suppression of forward dilepton production [22].

VI. OUTLOOK

In this paper we have formulated the general structure of the spectral functions that describe the rate of virtual photon (dilepton) production in a heavy ion collision that is locally anisotropic in momentum space. As we have demonstrated, momentum-space anisotropy induces new angular dependence in the transverse structure functions and, in the case of a non-parity symmetric momentum-space anisotropy, a new structure function ρ_n appears. As an example, we delineated the formalism for the leading-order Drell-Yan process. The structure derived is not limited simply to production of virtual photons from a quark-gluon plasma, but encompasses all virtual photon production processes in collisions.

With this full framework in place for relating polarization information in dilepton production to the underlying physical mechanisms, the next step will be to generalize prior calculations for real photon production in an anisotropic quark-gluon plasma [18, 19]; also [8]. A forthcoming publication will present a detailed calculation of the polarization of dileptons to order α_s , the strong interaction fine structure constant, including Compton scattering of a gluon on a quark or antiquark to a virtual photon, and annihilation of a quark-antiquark pair into a gluon and virtual photon [24]. In the computation of the spectral functions, we include space and time dependent anisotropic quark, antiquark, and gluon distributions, hard thermal loops, and soft scale processes, with the space-time evolution described by full 3+1 dimensional anisotropic hydrodynamics.

Acknowledgments

We are grateful to Dr. Y. Akiba for very helpful conversations about dilepton production; to Prof. H. Specht for discussions of the NA60 experiment, to Dr. B. Friman and his group for detailed comparisons of his group's work and ours, and to the ECT* in Trento, which hosted the workshop on “New perspectives on Photons and Dileptons in Ultrarelativistic Heavy-Ion Collisions at RHIC and LHC” where we had valuable discussions. We thank the RIKEN iTHES Project and iTHEMS Program for partial support during the course of this work. This research was also supported in part by NSF Grant PHY1305891, JSPS Grants-in-Aid No. 25287066, and DOE Grant No. DE-SC0013470. We thank the Aspen Center for Physics, supported in part by NSF Grant PHY1066292, where this paper was partially written.

-
- [1] A. Adare *et al.* [PHENIX Collaboration], Phys. Rev. Lett. **104**, 132301 (2010), Phys. Rev. C **81**, 034911 (2010), Phys. Rev. C **91**, 064904 (2015).
 - [2] L. Adamczyk *et al.* [STAR Collaboration], arXiv:1607.01447 [nucl-ex].
 - [3] J. Adam *et al.* [ALICE Collaboration], Phys. Lett. B **754**, 235 (2016).
 - [4] P. Hoyer, Phys. Lett. B **187**, 162 (1987).
 - [5] E. L. Bratkovskaya, O. V. Teryaev and V. D. Toneev, Phys. Lett. B **348**, 283 (1995).
 - [6] E. Shuryak, arXiv:1203.1012 [nucl-th].
 - [7] Reviewed in Proc. XXV Int. Conf. on ultrarelativistic nucleus-nucleus collisions, Nucl. Phys. A Nucl. Phys. A 956, (2016).
 - [8] G. Baym and T. Hatsuda, PTEP **2015**, no. 3, 031D01 (2015).
 - [9] J. C. Collins and D. E. Soper, Phys. Rev. D **16**, 2219 (1977).
 - [10] C. S. Lam and W. K. Tung, Phys. Rev. D **18**, 2447 (1978); Phys. Rev. D **21**, 2712 (1980).
 - [11] J. C. Peng, W. C. Chang, R. E. McClellan and O. Teryaev, Phys. Lett. B **758**, 384 (2016).
 - [12] R. Arnaldi *et al.* [NA60 Collaboration], Phys. Rev. Lett. **102**, 222301 (2009).
 - [13] P. Romatschke and M. Strickland, Phys. Rev. D **68**, 036004 (2003).
 - [14] E. Speranza, M. Zétényi, and B. Friman, Phys. Letters B **764**, 282 (2017).
 - [15] M. E. Carrington, A. Gynther and P. Aurenche, Phys. Rev. D **77**, 045035 (2008).
 - [16] M. Laine, PoS CPOD 2014, 065 (2015). [arXiv:1502.05796 [hep-ph]].
 - [17] M. Strickland, Pramana **84**, no. 5, 671 (2015).
 - [18] B. Schenke and M. Strickland, Phys. Rev. D **76**, 025023 (2007).
 - [19] L. Bhattacharya, R. Ryblewski and M. Strickland, Phys. Rev. D **93**, no. 6, 065005 (2016).
 - [20] M. Martinez and M. Strickland, Phys. Rev. Lett. **100**, 102301 (2008).
 - [21] M. Martinez and M. Strickland, Phys. Rev. C **78**, 034917 (2008).
 - [22] M. Martinez and M. Strickland, Eur. Phys. J. C **61**, 905 (2009).
 - [23] R. Ryblewski and M. Strickland, Phys. Rev. D **92**, no. 2, 025026 (2015).
 - [24] G. Baym, T. Hatsuda, A. Ipp, and M. Strickland, forthcoming.
 - [25] S. Jeon and U. Heinz, in *Quark-Gluon Plasma 5* (World Scientific Publ. Co., Singapore 2016), pp. 131-187.
 - [26] M. Strickland, Acta Phys. Polon. B **45**, no. 12, 2355 (2014).